Thermally reversible band bending for Bi/GaAs(110): Photoemission and inverse-photoemission investigations

G. D. Waddill, C. M. Aldao, C. Capasso, P. J. Benning, Yongjun Hu, T. J. Wagener, M. B. Jost, and J. H. Weaver
Department of Chemical Engineering and Materials Science, University of Minnesota, Minneapolis, Minnesota 55455
(Received 20 November 1989)

Results of synchrotron-radiation photoemission, inverse-photoemission, and low-energy electron diffraction studies of the Bi/GaAs(110) interface over the temperature range 20 to 300 K are presented. At 300 K, the first Bi monolayer grows in zigzag chains along the $[1\bar{1}0]$ direction to form an ordered (1×1) overlayer. This overlayer is semiconducting with a gap of 0.7 eV. Continued deposition results in Bi island growth atop the initial monolayer (ML) and conversion from semiconducting to semimetallic character. Bi deposition at 50 K results in layer-by-layer growth with no long-range order. Temperature- and coverage-dependent studies of band bending show symmetric behavior for n- and p-type GaAs(110) with matched bulk dopant concentrations. For 300-K deposition, the Fermi level E_F moves rapidly toward final positions 0.74 and 0.98 eV below the conduction-band minimum for n- and p-type GaAs doped at 10^{17} cm^{-3}. For 50-K deposition, the bands remain nearly flat to coverages of 1–2 ML where E_F moves rapidly toward midgap. Significantly, both techniques also show that Fermi-level movement is thermally reversible, such that the position of E_F in the surface band gap depends on temperature. A small part of the E_F movement is due to nonequilibrium processes involving the creation of electron-hole pairs by the incident photon or electron beam followed by the transport of the minority carriers to the surface region by the electric field in the depletion region. This surface voltage is most important at low temperature, and studies which vary the incident photon flux by over 3 orders of magnitude establish that the photovoltage has a small (≤ 100 meV), but non-negligible, effect on the band bending measured under "normal" experimental conditions. Hence, equilibrium processes control coupling of substrate and adsorbate-induced states in the GaAs band gap through the semiconductor depletion region and they determine the temperature-dependent interface band bending.

I. INTRODUCTION

Ordered, nondisruptive overlayers provide an opportunity to correlate structural and electronic properties of metal-semiconductor interfaces. To date, only Sb and Bi are known to form such overlayers on GaAs(110). The Sb/GaAs(110) system has been extensively studied,[1–6] and even the recently discovered Bi overlayer has been the subject of a number of investigations.[7–10] These studies have established that one monolayer (ML) of Bi grown on GaAs(110) at 300 K forms an ordered (1×1) overlayer consisting of Bi zigzag chains along the $[1\bar{1}0]$ direction accompanied by an ordered array of vacancies to relieve strain in the ordered Bi terraces (lattice mismatch $\sim4\%$). This Bi monolayer is semiconducting, but further Bi deposition results in the formation of Bi islands atop the first Bi layer, and the overlayer becomes semimetallic. The experimental techniques used to date to probe the interface include angle-integrated and angle-resolved photoemission,[7,9] scanning tunneling microscopy (STM),[9] low-energy electron diffraction (LEED),[7–10] and angle-resolved inverse photoemission.[8,10]

The present study combines synchrotron-radiation photoemission, angle-resolved inverse photoemission, and LEED to examine the temperature-dependent evolution of the Bi-GaAs(110) interface. We find that deposition of Bi at 50 K fails to produce long-range order, but that the interface is still abrupt and nondisrupted. Furthermore, we see temperature-dependent band-bending evolution that is symmetric at all temperatures for n- and p-type GaAs when the bulk doping concentrations are matched. These results are consistent with recent findings for metal-GaAs interfaces.[11] We observe, for the first time with both photoemission and inverse photoemission, that the amount of band bending depends reversibly on temperature for a semiconducting overlayer. Specifically, the Fermi level (E_F) is located ~150 meV from the conduction-band minimum (CBM) or valence-band maximum (VBM) for n- and p-type substrates when 1 ML of Bi is deposited at 50 K. Warming results in E_F movement toward midgap, but cooling restores the surface Fermi-level position to the 50-K position. This observation for a semiconducting overlayer is analogous to that reported for a number of metal-GaAs(110).[12] Aldao *et al.*[13] explained this temperature-, dopant-concentration, and coverage-dependent movement of E_F by emphasizing the coupling through the semiconductor depletion region of semiconductor bulk states near the CBM (or VBM) with adatom-induced gap states at the surface.[11–13]

An important point established in this paper is that

part of the band bending measured with photoemission and inverse photoemission is due to the measurement technique itself. In particular, flux-dependent studies demonstrate that E_F moves toward the band extrema (toward flat-band conditions) when the flux is increased. This suggests that production of electron-hole pairs by the incident particles (either electrons or photons) and the subsequent transport of minority carriers to the surface region moves the measured E_F from its equilibrium position. This nonequilibrium effect has been observed to flatten the bands for Si(111) and at metal-Si(111) interfaces at low temperature.[14,15] Here, we show that the incident photons in synchrotron studies produce a surface photovoltage (SPV), and experiments which vary the incident-photon-flux intensity by more than 3 orders of magnitude demonstrate that this surface-photovoltaic effect is most pronounced at low temperature and low coverage for Bi/GaAs(110). Significantly, this SPV effect accounts for only a small part of the observed temperature-dependent Fermi-level movement (65 meV compared to a total of $\sim$400 meV band bending at $\Theta=1$ ML). Hence, the observed temperature- and dopant-concentration-dependent band bending can be understood to arise from a combination of the nonequilibrium SPV and the equilibrium coupling of the substrate and the adsorbate-induced surface states.

II. EXPERIMENTAL PROCEDURES

Synchrotron-radiation photoemission measurements were performed at the Wisconsin Synchrotron Radiation Center using the Minnesota–Argonne–Los Alamos extended-range grasshopper monochromator and beamline. Core-level energy-distribution curves (EDC's) were collected using a double-pass cylindrical mirror analyzer in an ultrahigh-vacuum system described in detail elsewhere.[16] Overall instrumental resolution for Ga and As 3*d* core-level spectra was maintained at $\sim$200 and $\sim$250 meV, respectively. Photon energies of 40 and 65 eV for Ga 3*d* and 58 and 90 eV for As 3*d* were used to vary the probe depth (3 times the photoelectron mean free path) from $\sim$10 to $\sim$20 Å. Analysis of the EDC's was done using a nonlinear-least-squares-minimization curve-fitting routine.[17]

The samples were cleaved at 300 K at $\sim 5\times10^{-11}$ Torr. The copper sample holders to which the GaAs posts were mounted were then inserted into a copper tank attached to the second stage of a closed-cycle He refrigerator. Thermal contact between the sample holder and tank was provided by *in situ* Ga soldering. A tungsten filament served as a heater to melt the Ga in a recess designed to accommodate the copper sample holders. The sample holders were then soldered in place as the sample cooled. This process is straightforward and has the advantage of compromising neither the pressure nor the base temperature. Sample temperature was monitored with a Au-Fe/Chromel thermocouple attached to the copper tank, with calibration experiments indicating no difference between tank and sample temperatures. A tungsten heater allowed establishment of stable temperatures over the range $20 \le T \le 350$ K.

The inverse-photoemission spectroscopy (IPES) experiments were performed with an ultrahigh-vacuum spectrometer optimized for both ultraviolet- and x-ray-photoemission studies.[18] This system is also equipped with four-grid LEED optics for surface structural characterization. A highly collimated monoenergetic electron beam was directed onto the sample surface from an electron gun having a (1×5)-mm^2 planar BaO cathode and Pierce-type geometry. The emitted photons were dispersed with a near-normal-incident grating monochromator to be collected with a position-sensitive detector. The combined energy resolution depended on photon energy and varied between 0.3 and 1.0 eV for photons with energies between 10 and 40 eV. Electron-momentum resolution for the **k**-resolved (KRIPES) experiments was better than 0.1 Å^{-1}. Angle-dependent studies were performed by varying the angle between the incident electron beam and the sample surface normal between 0° and 45° while maintaining the angle between the incident electron beam and the outgoing photon beam at 60°.

In the IPES studies, sample temperatures of $\sim$50 K were achieved by attaching the sample to a copper cold finger mounted on a copper braid secured to the second stage of a closed-cycle He refrigerator. The temperature was again monitored with a Au-Fe/Chromel thermocouple mounted on the sample holder. The samples were cleaved at 300 K and then attached to the cold finger at pressures of $\sim 8\times10^{-11}$ Torr.

In both systems, Bi was evaporated from resistively heated tungsten boats onto clean *n*-type (Si doped at 1×10^{17} cm^{-3}) and *p*-type (Zn doped at 1×10^{17} cm^{-3}) GaAs(110) surfaces prepared by *in situ* cleaving. Stable evaporation rates monitored with calibrated quartz-crystal microbalances located near the samples were established prior to exposure to the Bi flux. The system pressures did not exceed 4×10^{-10} Torr during deposition. Adatom exposures are expressed here in monolayer (ML) units, with 1 ML or 8.85×10^{14} atoms/cm^2 corresponding to $\sim$3.15 Å of Bi. Uniform coverages are not necessarily implied.

III. RESULTS AND DISCUSSION

As noted above, the structural and electronic properties of the Bi/GaAs(110) interface formed at 300 K are well documented.[7–10] In the following we present the salient features of the Bi/GaAs(110) interface formed at both 50 and 300 K. We then discuss temperature-dependent band bending to demonstrate the importance of equilibrium and nonequilibrium processes in determining the electrical properties of the interface.

A. Interface structure

Figure 1 shows Ga 3*d* (left) and As 3*d* (right) core-level energy-distribution curves (EDC's) following Bi deposition at 300 K. These spectra have been background subtracted and normalized to constant height to emphasize line-shape differences. The two components observed for the clean surface correspond to emission from atoms in the bulk (labeled 1) and atoms at the relaxed surface (la-

beled 2). Deposition of Bi results in the loss of the surface component for both core levels by ~ 1 ML (3 Å). For the Ga 3*d* EDC's, loss of the surface component is accompanied by the growth of a third component (labeled 3) at 0.25 eV lower binding energy than the bulk component. This feature is due to emission from Ga atoms bonded to Bi atoms. It grows in relative intensity to a coverage of ~ 1 ML as the conversion of Ga atoms at the free relaxed GaAs(110) surface to Ga atoms bonded to Bi is completed. For coverages ≥ 1 ML, this Bi-Ga component persists with the same relative intensity, consistent with a layer of Ga atoms bonded to the first monolayer of Bi atoms. For the As 3*d* EDC's, no Bi-induced components can be resolved. Although Bi grows in zigzag chains along the [1$\bar{1}$0] direction for submonolayer coverages,[7-10] it is apparent that Bi—As bonding at the interface results in an As 3*d* binding energy that is at the same (or nearly the same) energy as that for bulk As atoms.

Further evidence for Bi—As bonding is provided in Fig. 2, which shows Bi 5*d* EDC's for Bi deposition at 300 K (left) and 50 K (right). For 300-K deposition and $\Theta \leq 1$ ML, the EDC's are fitted with two components of equal intensity separated by 0.36 eV. This is consistent with the results of Joyce *et al.*[7] and Ludeke *et al.*,[9] who attributed the two components to Bi bonded to surface Ga and surface As atoms. At 50 K these two components have an intensity ratio of approximately 7:3, with the low-binding-energy component having the larger intensity at all Bi coverages. As will be discussed shortly, substrate core-level fits for 50-K Bi deposition make it possible to attribute the higher-binding-energy component to Bi bonded to As and the lower-binding-energy component to Bi bonded to Ga, in agreement with Ref. 9 but not with Ref. 7.

For $\Theta \geq 1$ ML, a third Bi component at 0.20 eV lower relative binding energy than the Bi-Ga component grows to dominate the spectra above 2 ML. This feature can be attributed to Bi bonded to Bi in the growing overlayer, consistent with the fitting proposed by Joyce *et al.*[7] In contrast, Ludeke *et al.*[9] used only two components separated by 0.36 eV to fit the Bi EDC's at all coverages, except between 1 and 3 ML, where a third feature of unknown origin on the high-binding-energy side of the spectra was required for a satisfactory fit. We suggest that this feature is an artifact of a two-component fit which does not separate the emission from Bi atoms in their three distinct bonding configurations (Bi—Ga, Bi—As, and Bi—Bi). We adopt the three-component fit proposed by Joyce *et al.*[7] because it provides a description of the interface at all Bi coverages while recognizing that Bi—Bi bonding need not result in a feature at the same energy

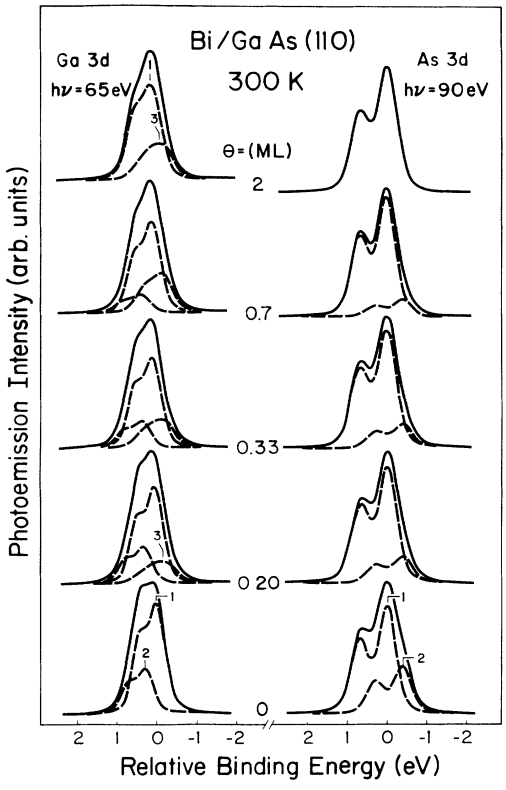

FIG. 1. Representative core-level EDC's for Bi deposition on GaAs(110) at 300 K. The Ga 3*d* EDC's show conversion of the surface component (feature 2) to emission associated with Ga bonded to Bi (feature 3). The As 3*d* EDC's show only the loss of the surface component as the overlayer develops, indicating that emission from Bi atoms bonded to As is energetically degenerate with bulk As (feature 1).

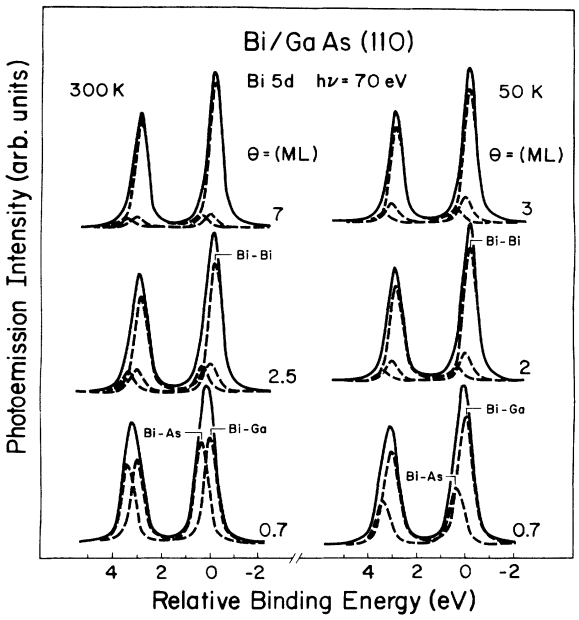

FIG. 2. Representative Bi 5*d* core-level EDC's for Bi deposition on GaAs(110) at 300 K (left) and 50 K (right). Submonolayer coverages show two features separated by 0.36 eV. The higher-binding-energy component is due to Bi bonded to As and the other arises from Bi bonded to Ga. At 300 K there is no preferred binding site as the thermal activation overcomes the preference for Bi—Ga bonding reflected by the 50-K spectra. At both temperatures a third component due to Bi—Bi bonding grows to dominate the spectra for $\Theta \geq 2$ ML.

as Bi—Ga surface bonding. At the highest coverages ($\Theta = 7-10$ ML), single-component fits of the Bi 5*d* EDC's were unsatisfactory, as previously concluded,[7,9] and it is evident that emission from Bi bonded to Ga and As atoms contributes to the dominant Bi-Bi emission. Finally, we stress that all of the core-level EDC's suggest an abrupt interface with no evidence of substrate disruption.

In Fig. 3 we show substrate core-level attenuation curves for Bi/GaAs(110) interface formation at 300 and 50 K. Total emission intensities were normalized to the total emission from the clean surface, $[I(\Theta)/I(0)]$, and plotted on a logarithmic scale. For Bi deposition at 50 K there is exponential attenuation ($1/e$ length of ~ 1 ML) indicative of layer-by-layer Bi growth. Bi deposition at 300 K again shows exponential attenuation until ~ 1 ML, but slower attenuation at higher coverage. This is consistent with Bi clustering in a Stranski-Krastanov growth mode.[7-10]

The Ga 3*d* EDC's following Bi deposition at 50 K are identical to those following 300-K deposition. This indicates the formation of equivalent Bi—Ga bonds and the loss of the Ga surface component at both temperatures. However, for the As 3*d* EDC's a component on the low-binding-energy side of the bulk emission persists to high coverages at 50 K. Since Bi—As bonding produces a feature in the As EDC's at the same energy as the bulk As feature, we conclude that this additional feature at 50 K is due to As that is *not bonded* to Bi, but is influenced by the presence of Bi at the interface. Furthermore, the relative intensity of this component ($\sim 20\%$ of the total As emission at $\Theta \geq 1$ ML) is less than would be expected if none of the As atoms at the interface were bonded to Bi. In contrast, the Bi—Ga bonding component is $\sim 35\%$ of the total Ga emission above 1 ML. This demonstrates that Bi—As bonding at the interface is not absent, but that half of the As surface atoms are bonded to Bi. Further evidence for this hypothesis is provided by the Bi 5*d* EDC's. Following deposition at 50 K, the Bi spectra are fitted by two interface components of *unequal* intensities. Since the As EDC's suggest that not all surface As atoms are bonded to Bi, we conclude that the lower-relative-intensity component in the Bi EDC's is due to Bi—As bonding. From Fig. 2, the weaker component is the Bi component at highest binding energy and is due to emission from Bi bonded to As. Consequently, the lower-binding-energy component of the two interface Bi features is due to Bi bonded to Ga. This is in agreement with the assignments made by Ludeke *et al.*[9] based on their results at 300 K. It suggests that there is a preferred binding site for Bi at the surface (Bi—Ga) but that the thermal energy at 300 K is sufficient to overcome this preference and distribute the Bi adatoms uniformly among As and Ga bonding sites. At 50 K the available thermal energy cannot distribute the Bi adatoms uniformly across the surface and, as a result, the Bi is preferentially bonded to Ga.

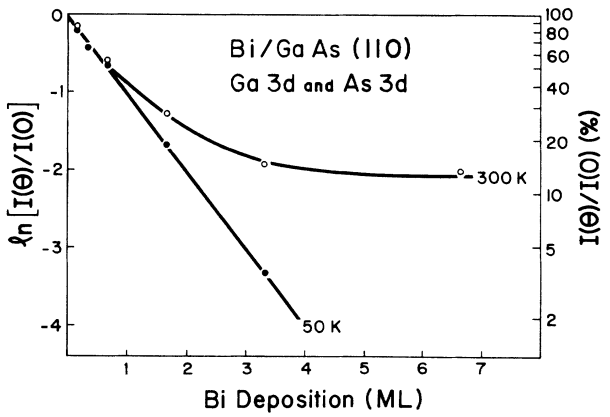

FIG. 3. Substrate core-level attenuation plots, $\ln[I(\Theta)/I(0)]$, for Bi deposition at 300 and 50 K. At 50 K the attenuation is exponential and indicates layer-by-layer Bi growth. At 300 K the first monolayer grows uniformly, but subsequent Bi deposition results in Bi-cluster formation atop this layer, as evidenced by the slower attenuation rate after 1 ML.

In order to gain additional insight into the details of Bi growth on GaAs(110), we investigated the Bi/GaAs(110) interface using inverse photoemission and LEED.[8] A sharp (1×1) LEED pattern was observed for Bi coverages ≤ 1 ML at 300 K. At higher coverages, extra diffraction spots were observed along the $[1\bar{1}1]$ and $[1\bar{1}\bar{1}]$ directions. However, there is an absence of every sixth LEED spot with periodicity in the $[1\bar{1}0]$ direction (Ref. 8). The missing diffraction spots along these directions are due to misfit dislocations resulting from distortions due to the differing Bi—Bi, Bi—Ga, and Bi—As bond lengths. The periodicity of the missing diffraction spots suggests a misfit dislocation every ~ 24 Å, in agreement with STM results, which revealed stress-induced Bi-island boundaries.[9] This pattern persisted to coverages as high as 50 Å.

Representative KRIPES photon-distribution curves (PDC's) for normal-incidence electrons for $0 \leq \Theta \leq 10$ ML are shown in Fig. 4 together with photoemission valence-band spectra. The KRIPES spectra were taken with an incident energy of 16.25 eV. They have been normalized to electron flux and spectral throughput of the optical system. The photoemission spectra obtained with a photon energy of 65 eV were normalized to constant height. There is no unique normalization of the IPES and PES spectra, and no relative-intensity information between the two sets of spectra is intended. For ~ 1 ML Bi, a strong Bi-derived empty state (labeled *B* and hatched) is observed 1.25 eV above E_F. Another Bi-derived state (labeled *A*) is observed ~ 0.35 eV above E_F for coverages > 1 ML. Increasing the Bi coverage results in the appearance of two other Bi-derived states (labeled *C* and *D*) at 2.7 and 3.7 eV above E_F as well as filling in of emission between features *A* and *B*. The results summarized in Fig. 4 establish that 1 ML of Bi on GaAs(110) is semiconducting with a band gap of 0.7 eV.[8] At 2 ML the overlayer becomes semimetallic and remains so to higher coverage.

Feature *B* in Fig. 4 is the first Bi-derived feature observed for deposition at 300 K. It is not discernible for $\Theta \leq 0.5$ ML, but is prominent at ~ 0.67 ML. Angle-resolved photoemission results following deposition of 1

ML Bi at room temperature showed the dispersion of feature B along the Bi zigzag-chain-growth direction.[8] Feature B is therefore attributed to states resulting from Bi chain growth with delocalization along the chains. No dispersion was observed perpendicular to the chains, consistent with little chain-chain bonding. In contrast, deposition at 50 K produced emission near the energy of feature B, but it was broader, it extended further into the gap, and there was no dispersion in $\mathbf{k}$ space. We therefore envision the surface as disordered with what would likely be frustrated chain growth together with dispersed Bi atoms and aggregates. LEED results show that deposition at 50 K produced no long-range order. However, warming to 300 K provided thermal activation and facilitated chain growth. For the overlayer warmed to 300 K, we found behavior analogous to that for deposition at 300 K, namely a $p(1\times1)$ LEED pattern, band dispersion, and sharpening of the emission related to feature B. These observations are consistent with the photoemission results which established that Bi deposition at 50 K resulted in Bi bonding preferentially to Ga. While there is still some Bi—As bonding at the interface, it is inhibited and chain growth is not extensive.

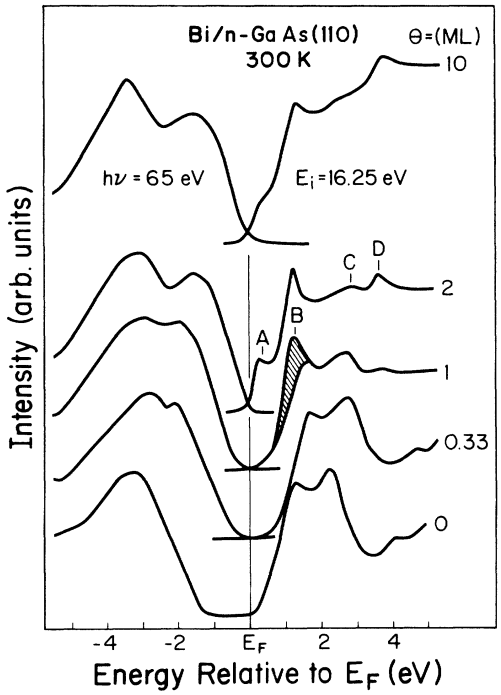

FIG. 4. Normal-incidence inverse-photoemission PDC's for 0–10 ML Bi on n-type GaAs(110) taken with $E_i = 16.25$ eV and photoemission EDC's taken with $h\nu = 65$ eV. A pronounced Bi-derived surface resonance (feature B) appears 1.25 eV above E_F for 1 ML coverage. It is associated with Bi zigzag chains and exhibits dispersion in $\mathbf{k}$ space corresponding to the [110] direction. For $\Theta \geq 2$ ML, Bi-derived features A, C, and D develop as the overlayer converts from a semiconductor to a semimetal.

The photoemission, inverse-photoemission, and LEED results establish that an abrupt Bi/GaAs(110) interface is formed at both 50 and 300 K. Growth of the Bi monolayer occurs in zigzag chains along the $[1\bar{1}0]$ direction with long-range $p(1\times1)$ order at 300 K, but no long-range order at 50 K. Differences may be due to the preference for Bi bonding to Ga, which is overcome at 300 K by the extra thermal energy which distributes the Bi adatoms uniformly between As and Ga binding sites. Once this occurs, there is an energy gain associated with Bi delocalization and chain formation. At 50 K, subsequent Bi growth occurs in a layer-by-layer fashion while Bi clusters form atop the monolayer at 300 K.

B. Band bending and temperature cycling

In the last three years, temperature-dependent band bending at metal-semiconductor interfaces has been the subject of considerable study.[11–13,19–22] Initially, it was observed that metal deposition on n- and p-type substrates at 300 K resulted in rapid and nearly symmetric movement of E_F toward midgap with the final E_F position achieved by 1–2 ML. At low temperatures (ranging from 50 to 200 K) the situation was initially found to be not so simple. For n-type substrates the substrate bands remained nearly flat to coverages between 1 and 2 ML. Above this threshold, E_F moved rapidly toward the final pinning position near midgap. For p-type substrates at low temperature, E_F moved more rapidly into the gap than at 300 K, often overshooting the final position observed at 1–2 ML. This low-temperature asymmetry was attributed to the formation of donor levels in the gap by isolated adatoms at low temperature. Overlayer metallization was believed to account for the high-coverage behavior when E_F moved into the gap for n-type GaAs and returned from the overshoot position for p-type GaAs.[23] The overshoot for p-type substrates at low temperature was attributed to increasing dipole interaction between adatoms as the coverage increased from submonolayer to the metallization limit.

More recently, systematic studies of temperature-dependent band bending for GaAs(110) with different bulk doping concentrations, N, established that the asymmetry was a manifestation of the different substrate doping concentrations used in the previous work.[11–13] Specifically, nearly flat bands were observed on both-n and p-type substrates following atom deposition at 60 K onto substrates with doping concentrations of 1×10^{17} cm^{-3} up to the metallization threshold. Symmetric E_F movement into the gap was then seen. For doping concentrations of $\sim1\times10^{18}$ cm^{-3}, E_F moved into the gap at much lower coverages for both n- and p-type GaAs(110). These results are consistent with those of earlier studies, since they had examined p-type samples with $N_A \geq 10^{18}$ cm^{-3} and n-type samples with N_D near 10^{17} cm^{-3}. This behavior, which cannot be explained by models that assume donorlike character for isolated adatoms, was observed for a wide range of different metal overlayers (including very reactive Ti, moderately reactive Co, and weakly reactive Ag). Hence, the results are largely in-

dependent of the chemical or morphological structure at the interface. We conclude that E_F evolution is symmetric at all temperatures for n- and p-type substrates with matched doping concentrations.

The following extends the generality of the above observations for metal-GaAs(110) interfaces to the Bi/GaAs(110) interface for which 1 ML of Bi is semiconducting but ≥ 2 ML is semimetallic. In Fig. 5 we show the Fermi-level position as a function of coverage for growth at 50 and 300 K on n- and p-type GaAs(110) with $N_A = N_D = 1 \times 10^{17}$ cm^{-3}. Clearly, symmetric E_F movement is observed at both temperatures. At 300 K, E_F moves rapidly toward its final position 0.74 and 0.98 eV below the CBM for n- and p-type GaAs, respectively. At 50 K, nearly flat bands are observed until ~ 2 ML, when E_F moves rapidly toward its final position. The 50-K results to not present the final Fermi-level position because rapid substrate attenuation prohibited measurements at high coverages ($1/e$ attenuation length of 1 ML). The behavior shown in Fig. 5 is analogous to that reported for metal-GaAs(110) interfaces and can be understood in terms of the dynamic coupling model.[13] This model relates band-bending differences to the temperature and dopant-concentration dependences of the coupling of bulk states near the band extrema outside the depletion region with adsorbate-induced surface gap states. The temperature dependence arises from the thermal distribution of electrons (holes) in the conduction (valence) band, and the dopant dependence arises from the depletion-region width. For heavily doped samples the depletion width is smaller for the same amount of band bending, and surface-to-bulk coupling is facilitated, compared to lightly doped samples. Coupling can be viewed as the overlap of bulk and adatom-induced wave functions. In the absence of such overlap there can be no net accumulation of charge in the surface region and no band bending occurs. The dynamic coupling is strictly applicable in the low-coverage regime before significant delocalization of adatom-induced states at the surface produces a continuum of gap states. The results of Fig. 5 for Bi/GaAs(110) can be understood in this manner.

One consequence of the dynamic coupling model is that, in the absence of significant morphological or chemical changes at the interface, E_F movement should be reversible with temperature. In Fig. 6 we summarize results of temperature-cycling experiments for 1 ML Bi on p-type GaAs ($N_A = 1 \times 10^{17}$ cm^{-3}). In order to avoid morphological changes, the Bi was deposited at 300 K to produce an ordered semiconducting overlayer and the samples were then cooled. Reheating to 300 K (not shown) established that the Fermi-level movement was completely reversible with temperature. For the photoemission results (circles), we plot relative binding-energy shifts for the substrate core levels (solid circles) as well as for the Bi overlayer (open circles). The core levels (both substrate and overlayer) were all recorded at the same photon energy ($h\nu = 65$ eV), so that the only experimental parameter varied was the temperature. The energy references are the core-level binding energies at 300 K.

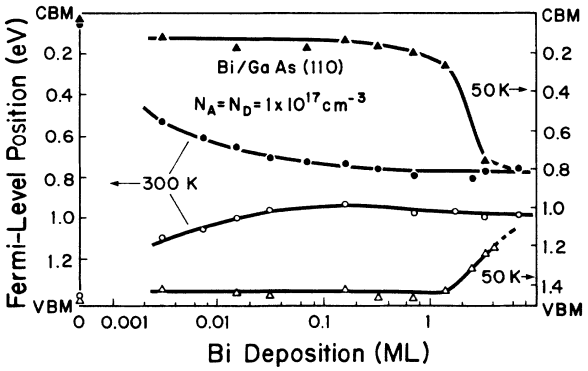

FIG. 5. Fermi-level movement as a function of Bi deposition for n- and p-type GaAs(110) doped at 10^{17} cm^{-3} for 300 and 50-K deposition. The step toward midgap for both n- and p-type GaAs at 50 K near 2 ML is due to overlayer conversion from semiconducting to semimetallic character and the consequent presence of a continuum of states in the GaAs band gap (see Fig. 4). The enhanced band bending at every coverage at 300 K is a consequence of the improved surface-to-bulk coupling at higher temperatures.

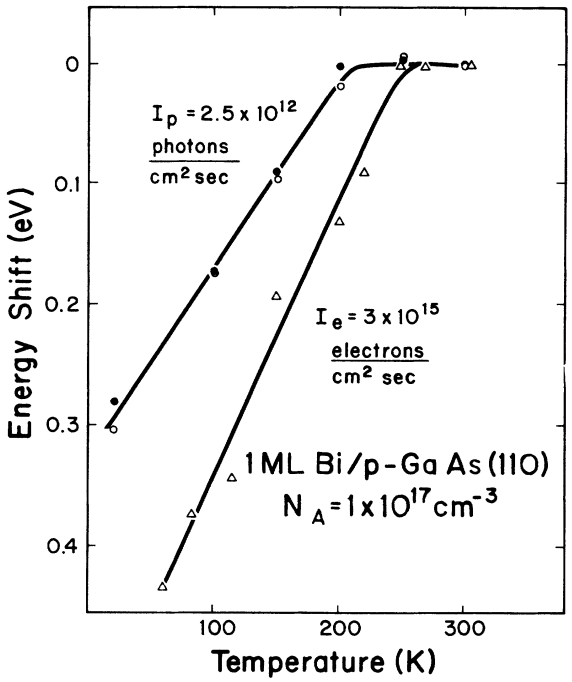

FIG. 6. E_F shift for 1 ML Bi [p-type GaAs(110)] with $N_A = 10^{17}$ cm^{-3} as a function of temperature and incident particle. The circles were obtained from analysis of the photoemission results and the triangles were derived from IPES results. The shifts in E_F were fully reversible with temperature. The larger observed E_F shifts for the IPES experiments were due to the greater incident flux since the incident particles produce electron-hole pairs which can be separated within the depletion region. Minority-carrier accumulation at the surface results in nonequilibrium flattening of the bands.

The substrate data represent an average of the Ga and As $3d$ shifts and are accurate to ± 20 meV. The results show no change in binding energy (and, hence, E_F position) between 200 and 300 K. Below 200 K, E_F decreases linearly by ~ 300 meV at 20 K as the band bending is decreased and more nearly-flat-band conditions are established. The shift for the Bi $5d$ core level lies along the same curve since the Bi levels follow the substrate band bending and are referenced to intrinsic semiconductor levels rather than E_F. In Fig. 6 we also show results for E_F movement deduced from inverse-photoemission spectra. These were obtained by measuring the energy shift of feature B (related to Bi-chain formation) of Fig. 4. The results show qualitatively similar trends with the Fermi-level position unchanged between 250 and 300 K and decreasing linearly by ~ 430 meV at 60 K. This effect was again fully reversible, and equivalent results were observed on n-type substrates. Furthermore, the effect was seen on more heavily doped substrates ($\sim 10^{18}$ cm^{-3}). In this case, the total E_F movement was not as large because the depletion width was smaller and the barrier it represents was more transparent (~ 250 meV for 1 ML between 60 and 300 K).

It is interesting to note that the incident photon flux was $\sim 2.5\times 10^{12}$ cm^{-2} sec^{-1} in the photoemission experiments, while the incident electron flux was approximately 3 orders of magnitude greater for the IPES experiments. This suggests that some of the effect observed in Fig. 6 and in previous low-temperature studies[11–13] may be due to incident-beam effects. Higher incident flux will result in the production of more electron-hole pairs with the minority carriers driven to the surface region by the fields in the depletion region. This nonequilibrium process tends to flatten the bands and is more important at low temperatures. Such effects have been reported for Si(111) clean surfaces as well as for metal overlayers on Si(111).[14,15]

In order to investigate this surface-voltage effect more thoroughly, we performed synchrotron-radiation photoemission experiments for (1 ML Bi/[p-type GaAs(110)] for photon fluxes varying from 2.5×10^{9} to 2.5×10^{12} cm^{-2} sec^{-1}, as well as with illumination from an external lamp. Curves (a)–(c) in Fig. 7 are for photon fluxes of 2.5×10^{10}, 2.5×10^{11}, and 2.5×10^{12} cm^{-2} sec^{-1}, with curve (c) corresponding to the photon flux used in obtaining the data presented in Fig. 6. Again, the photon energy was held fixed at 65 eV. The flux was changed using the monochromator slits and by inserting Al filters into the beam path. Calibration experiments performed for unpinned clean GaAs(110) surfaces established that these procedures did not affect the measured binding-energy positions due to any experimental artifact.

The results of Fig. 7 show that there was no dependence on the synchrotron photon flux for $T \geq 200$ K, thus establishing that the surface-photovoltaic (SPV) effect is not important at these temperatures for this dopant concentration and coverage. At lower temperatures, however, flux dependences were more apparent. Specifically, the total E_F movement between 20 and 300 K is 282 meV at 2.5×10^{12} cm^{-2}sec^{-1}, 250 meV at 2.5×10^{11} cm^{-2}sec^{-1}, and 225 meV at 2.5×10^{10} cm^{-2}sec^{-1}. Measurements at 20 K with a photon flux of 2.5×10^{9} cm^{-2}sec^{-1} (the large square in Fig. 7 that overlaps the smaller solid square) establish that further reduction of the photon flux no longer moves E_F. We conclude that the SPV can be neglected for fluxes below 10^{10} cm^{-2}sec^{-1}. We also show the effect of illuminating the sample with an external lamp while collecting data with a photon flux of 2.5×10^{12} cm^{-2}sec^{-1}. The lamp has no effect at 300 K, but the bands were flattened significantly at lower temperature, indicating that saturation SPV had not been achieved using only the synchrotron photon flux. The amount of band flattening observed at low temperatures with the lamp is less than that observed in the IPES experiments where the incident electron flux is relatively high. This shows that nonequilibrium processes are more important in interpreting the IPES results.

The results of this study indicate that part, but not all, of the low-coverage temperature-dependent band-bending effects presented in Fig. 5 can be attributed to a surface voltage established by the photon (or electron) flux. From Fig. 7, the band bending for 1 ML Bi on p-type GaAs(110) with no SPV deviates from that measured with normal photon fluxes by only 65 meV at 50 K. This indicates that the SPV effect must be considered when

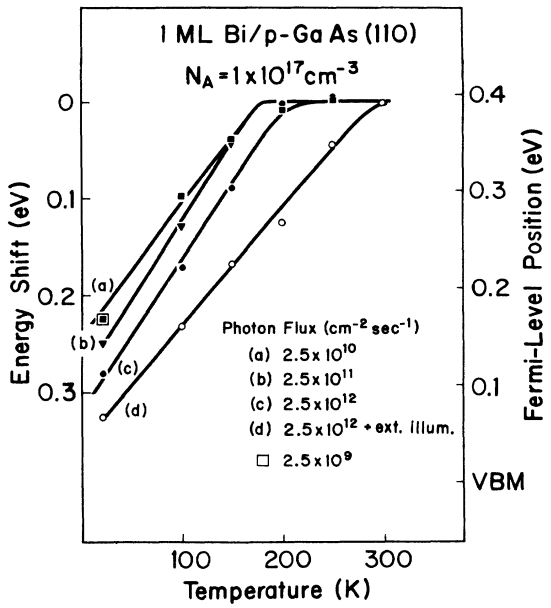

FIG. 7. E_F shift for 1 ML Bi [p-type GaAs(110)] with $N_A = 10^{17}$ cm^{-3} as a function of both temperature and photon flux. At 300 K there is no variation in E_F with photon flux, but increasing flux tends to flatten the bands as the temperature is decreased. While important, this surface-photovoltaic effect is small even at 20 K, where decreasing the flux by 3 orders of magnitude from normal experimental values ($\sim 10^{15}$ photons cm^{-2}sec^{-1}) increases the measured band bending by only ~ 60 meV. These results show that the SPV effect is more important at low temperatures, but that it represents only a small correction to the temperature-dependent band-bending results of Fig. 5.

measuring band bending at low temperatures. It also shows rather conclusively that most of the temperature-dependent movement of the Fermi level measured to date results from equilibrium processes that determine the coupling of the bulk and surface states through the semiconductor depletion region. These processes have been described in greater detail in Refs. 11–13.

IV. CONCLUSIONS

We have presented synchrotron-photoemission, inverse-photoemission, and LEED results characterizing the Bi/GaAs(110) interface in the temperature range 20–300 K. At 300 K our results are consistent with a number of other studies[7–10] that establish Bi-monolayer growth in chains along the $[1\bar{1}0]$ direction and the formation of an ordered (1×1) overlayer without substrate disruption. Subsequent Bi deposition results in three-dimensional Bi-island growth atop the first monolayer. The Bi overlayer is semiconducting with a gap of 0.7 eV for $\Theta \leq 1$ ML, but becomes semimetallic after ~ 2 ML. For deposition at 50 K, Bi grows in a layer-by-layer mode with no substrate disruption, but also with no long-range order. Temperature-dependent band-bending results for the semiconducting, ordered monolayer in which there is one-dimensional delocalization show symmetric E_F movement for n- and p-type substrates with matched dopant concentrations.[11–13] We also report, for the first time, reversible temperature E_F movement observed with both synchrotron-radiation photoemission and inverse photoemission, i.e., using photons and electrons as the probe. The results suggest that technique-related nonequilibrium processes such as the production of electron-hole pairs and the transport of minority carriers to the surface region are important in interpreting these results. Careful studies of the variation in band bending with changing photon flux establish that the surface photovoltage contributes in a non-negligible fashion to the results reported to date, but that it cannot account for all the observed temperature dependence. Instead, we conclude that equilibrium processes related to the coupling of the substrate to the surface through the depletion region outlined in Refs. 11–13 are primarily responsible for the observed temperature- and dopant-concentration-dependent effects on band bending. Our results establish that great care must be exercised to isolate the effects of equilibrium processes when studying Schottky-barrier formation at low temperatures and add further insight into the role of the parameters that determine band bending.

ACKNOWLEDGMENTS

This work was supported by the U.S. Office of Naval Research under Contracts No. N00014-87-K-0029 and No. N00014-86-K-0427. Stimulating discussions with J. Tersoff are gratefully acknowledged. The photoemission experiments were done at the University of Wisconsin Synchrotron Radiation Center (Stoughton, WI) a user facility supported by the U.S. National Science Foundation. The assistance of the staff of that laboratory is appreciated.

[1] P. Skeath, C. Y. Su, I. Lindau, and W. E. Spicer, J. Vac. Sci. Technol. **17**, 874 (1980).

[2] C. B. Duke, W. K. Ford, A. Kahn, and J. Carelli, Phys. Rev. B **26**, 803 (1982).

[3] P. Mårtensson, G. V. Hansson, M. Lähdeneimi, K. O. Magnusson, S. Wiklund, and J. M. Nicholls, Phys. Rev. B **33**, 7399 (1986).

[4] F. Schäffler, R. Ludeke, A. Taleb-Ibrahimi, G. Hughes, and D. Rieger, Phys. Rev. B **36**, 1328 (1987); J. Vac. Sci. Technol. B **5**, 1048 (1987).

[5] R. M. Feenstra and P. Mårtensson, Phys. Rev. Lett. **61**, 447 (1988), and Phys. Rev. B **39**, 7744 (1989).

[6] W. Drube and F. J. Himpsel, Phys. Rev. B **37**, 855 (1988).

[7] J. J. Joyce, J. R. Anderson, M. M. Nelson, C. Yu, and G. J. Lapeyre, J. Vac. Sci. Technol. A **7**, 859 (1989); Phys. Rev. B **40**, 10412 (1989).

[8] Y. Hu, T. J. Wagener, M. B. Jost, and H. Weaver, Phys. Rev. B **40**, 1146 (1989).

[9] R. Ludeke, A. Taleb-Ibrahimi, R. M. Feenstra, and A. B. McLean, J. Vac. Sci. Technol. B **7**, 936 (1989); B. M. Trafas, D. M. Hill, and J. H. Weaver (unpublished).

[10] A. B. McLean and F. J. Himpsel, Phys. Rev. B **40**, 8425 (1989).

[11] See, for example, C. M. Aldao, S. G. Anderson, C. Capasso, G. D. Waddill, I. M. Vitomirov, and J. H. Weaver, Phys. Rev. B **39**, 12977 (1989), and references therein.

[12] I. M. Vitomirov, G. D. Waddill, C. M. Aldao, S. G. Anderson, C. Capasso, and J. H. Weaver, Phys. Rev. B **40**, 3483 (1989).

[13] C. M. Aldao, I. M. Vitomirov, G. D. Waddill, S. G. Anderson, and J. H. Weaver, Phys. Rev. B (to be published).

[14] J. E. Demuth, W. J. Thompson, H. J. DiNardo, and R. Imbihl, Phys. Rev. Lett. **56**, 1408 (1986).

[15] K. Markert, P. Pervan, W. Heichler, and K. Wandelt, J. Vac. Sci. Technol. A **7**, 2873 (1989).

[16] C. M. Aldao, I. M. Vitomirov, F. Xu, and J. H. Weaver, Phys. Rev. B **37**, 6019 (1988).

[17] J. J. Joyce, M. del Giudice, and J. H. Weaver, J. Electron. Spectrosc. and Relat. Phenom. **49**, 31 (1989); I. M. Vitomirov, C. M. Aldao, Z. Lin, Y. Gao, B. M. Trafas, and J. H. Weaver, Phys. Rev. B **38**, 10776 (1988).

[18] Y. Gao, M. Grioni, B. Smandek, J. H. Weaver, and T. Tyrie, J. Phys. E **21**, 488 (1988).

[19] K. Stiles, A. Kahn, D. G. Kilday, and G. Margaritondo, J. Vac. Sci. Technol. B **5**, 987 (1987); K. Stiles, S. F. Horng, A. Kahn, J. McKinley, D. G. Kilday, and G. Margaritondo, J. Vac. Sci. Techol. B **6**, 1392 (1988).

[20] R. Cao, K. Miyano, T. Kendelewicz, K. K. Chin, I. Lindau, and W. E. Spicer, J. Vac. Sci. Technol. B **5**, 998 (1987); W. E. Spicer, R. Cao, K. Miyano, C. McCants, T. T. Chiang, C. J. Spindt, N. Newman, T. Kendelewicz, I. Lindau, E. Weber, and Z. Liliental-Weber, in *Metallization and Metal-Semiconductor Interfaces,* NATO Advanced Study Institute,

Series B, Vol. 195 edited by I. P. Batra (Plenum, New York, 1989).
[21]M. Prietsch, C. Laubschat, M. Domke, and G. Kaindl, Phys. Rev. B **38**, 10 655 (1988).
[22]G. D. Waddill, C. M. Aldao, I. M. Vitomirov, Y. Gao, and J. H. Weaver, J. Vac. Sci. Technol. A **7**, 865 (1989); Phys. Rev. Lett. **62**, 1568 (1989).
[23]M. Mönch, J. Vac. Sci. Technol. B **6**, 1270 (1988); J. E. Klepeis and W. A. Harrison, *ibid.* **7**, 964 (1989); I. Lefebvre, M. Lannoo, and G. Allan (unpublished).